N-terminal tail domains of core histones in nucleosome block the access of anticancer drugs, mithramycin and daunomycin, to the nucleosomal DNA

Mohd. Ayoub Mir, Suman Das, Dipak Dasgupta*

Biophysics Division, Saha Institute of Nuclear Physics, 37 Belgachhia Road, Calcutta700 037, India

Abstract

Mithramycin (MTR) and daunomycin are two anticancer drugs that bind reversibly to double stranded DNA with (G.C) base specificity leading to inhibition of transcription. MTR is a groove binder of DNA in the presence of a divalent cation such as Mg^{2+}, while daunomycin intercalates in the double stranded DNA structure. In order to understand the mechanism of action of the two types of transcription inhibitor, namely, groove binder and intercalator, we have studied the effect of N-terminal tail domains in histone proteins of the nucleosome upon the association of both MTR and daunomycin with the nucleosome core particle, because the tails modulate the accessibility to nucleosome during gene expression. Using a combination of spectroscopic, thermodynamic and biochemical studies, we have shown that N-terminal intact and chopped core particles interact differently with the same ligand and the N-terminal tail domains of core histones in the nucleosome stand in the way of free access of these ligands to the nucleosomal DNA. Tryptic removal of N-terminal tail domains of core histones enhances the binding potential and accessibility of both MTR and daunomycin to nucleosomal DNA. They disassemble the nucleosome structure leading to a release of DNA, N-terminal chopped nucleosomes being more susceptible for disruption compared to N-terminal intact nucleosomes. The extent of these effects is more pronounced in case of the intercalator daunomycin. Thus, N-terminal tail domains protect the eukaryotic genome from external agents, such as anticancer drugs, and the degree of protection is dependent upon the mode of binding to DNA.
© 2003 Elsevier B.V. All rights reserved.

Keywords: Anticancer drug; Mithramycin; Histone tail domains; Nucleosome core; Mithramycin–Mg^{2+} complexes

1. Introduction

Mithramycin (MTR, structure shown in Fig. 1a) is a member of the aureolic acid group of antitumor antibiotics from *Streptomyces plicatus*. It is clinically employed for testicular carcinoma and Paget's disease [1]. It consists of a chromomycinone moiety, the aglycon ring, either side of which is linked to six-member sugar residues such as D-mycarose, olivose and oliose via *O*-glycoside linkages [2] (Fig. 1a). It inhibits the expression of some proto-oncogenes like c-myc, having an important role in the regulation of cell proliferation
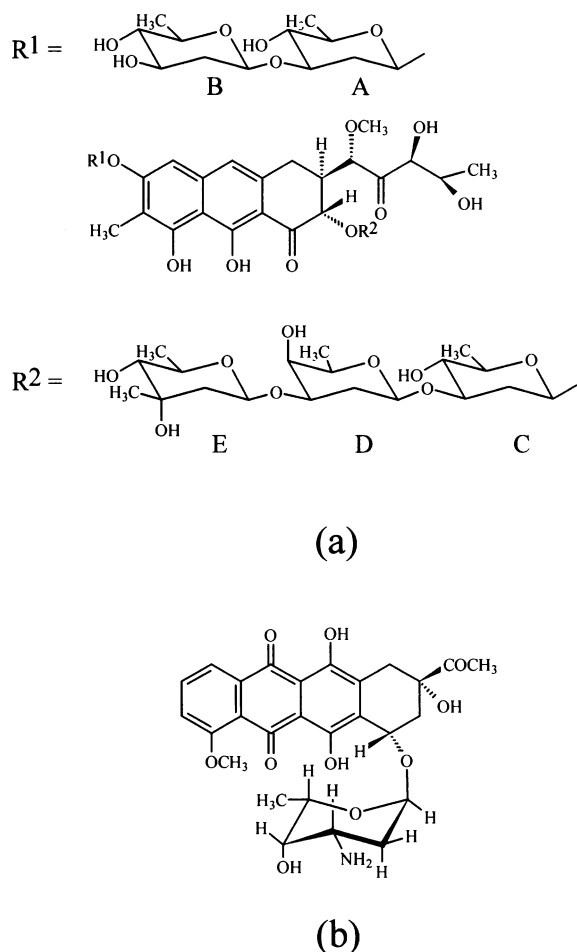
Fig. 1. Chemical structures of (a) MTR and (b) daunomycin.

and differentiation [3]. This antibiotic has been proposed as a neurological therapeutic for the treatment of diseases associated with aberrant activation of apoptosis [4]. Daunomycin (Fig. 1b), one of the anthracycline antibiotics, is among the most effective drugs for cancer chemotherapy. Anticancer properties of these antibiotics have been ascribed to its inhibitory role in DNA replication and RNA transcription process during macromolecular biosynthesis [1,2,5,6].

Chromosomal DNA is a cellular target of both MTR and daunomycin. Bivalent metal ions, such as Mg^{2+}, are an essential requirement for the (G.C) base-specific association of MTR at and above neutral pH [4,7,8]. Previous studies from our laboratory have shown that in the absence of DNA, MTR forms two different types of complexes with Mg^{2+} [9–11]. Stoichiometry of these complexes are 1:1 (complex I) and 2:1 (complex II) in terms of antibiotic–Mg^{2+}. These complexes are the potential DNA-binding ligands at and above physiological pH. Being structurally different, they bind with different energetics to the same DNA in the minor groove [9–11]. DNA-binding properties of the antibiotic have been very well studied in different laboratories [8–15]. From single crystal molecular structures, NMR and other spectroscopic studies, it has been demonstrated that daunomycin has a preference for the GC bases of DNA and intercalates in the GC base pairs [16–18].

In the cell, chromosomal DNA that serves as a binding site for the anticancer drugs is associated with histones and other non-histone chromosomal proteins. High-resolution structures of the nucleosome core particle [19,20] have shown that the two turns of the DNA super helix in the nucleosome core have the grooves aligned, creating sufficient gaps for the amino-terminal tails of both H2B and H3 histones to pass through to the outside of the core particle. H2A and H4 tails pass across the super helix on the flat faces of the particle to the outside as well. Exposed N-terminal tails of core histones are post-translationally modified by acetylation and phosphorylation during eukaryotic transcription. These modifications alter the charge distribution on the N-terminal tail [21,22]. The effect of these modifications upon epigenic regulation in eukaryotic system is becoming apparent [22]. The tail domains also prevent the access of transcription factors such as TFIIIA [23] and other DNA-binding proteins to the nucleosomal templates [24]. Apparently they have no role in the conformational or in the salt-dependent stability of the nucleosome core particle [25,26]. These studies imply that the nucleosome uses the N-terminal tails of core histones as a tool to handle the transcription machinery during eukaryotic gene expression. Recent studies have shown that nucleosomal DNA is surprisingly adaptable in accommodating sequence-specific DNA-binding ligands [21,27]. They allow the propagation of structural

deformations while maintaining the histone–DNA interactions.

As a part of our studies to understand the association of the aureolic acid group of antibiotics with different levels of chromatin structure, we earlier reported that the antibiotics interact with both linker and nucleosomal DNA in rat and chicken liver chromatin [28]. We also showed the role of core histone tail domains in the association of chromomycin A_3 with nucleosomes [29]. The objectives of the present study are as follows. We have extended our studies to understand the role of N-terminal tail domains upon the DNA-binding potential of MTR–Mg^{2+} complexes. MTR is used clinically and its potential as a drug is being reevaluated [4,30]. We have included another widely used anticancer drug, daunomycin, in this study to examine the potential of these drugs to disrupt nucleosomes and the role of N-terminal tail domains, if any, in the process. We want to know whether the two mechanistically distinct modes of DNA binding of MTR and daunomycin influence an association with and subsequent disassembly of normal and N-terminal chopped nucleosome core particles.

2. Materials and methods

2.1. Drugs and reagents

MTR, daunomycin, Tris, magnesium chloride solution (4.9 M), calcium chloride solution (1 M), proteinase K, phenylmethylsulfonyl fluoride, ethylenediaminetetraacetic acid disodium salt (EDTA), Triton-X-100, micrococcal nuclease, trypsin immobilized on agarose beads and calf thymus DNA were from Sigma Chemical Company, USA. The buffer was prepared in quartz distilled deionized water from Milli-Q source, Millipore Corporation, USA.

2.2. Preparation of nucleosome core and tryptic removal of N-terminal tail domains

Nucleosome core particles were isolated from male albino sprigo dowly rats as described in our earlier report [29]. The N-terminal tail domains of core histones were removed by limited proteolysis as described earlier [29].

2.3. Absorbance and fluorescence measurements

Absorption and fluorescence spectra were recorded with a Hitachi U-2000 spectrophotometer and a Shimadzu RF-540 spectrofluorometer, respectively. Concentrations of MTR and daunomycin were estimated from molar absorption coefficient value of 10 000 M^{-1} cm^{-1} at 400 nm and 11 500 M^{-1} cm^{-1} at 480 nm, respectively [10,31]. The fluorescence excitation wavelength was 470 nm for MTR in order to avoid photodegradation of the antibiotic [10]. For daunomycin, the fluorescence excitation wavelength was fixed at 480 nm. During fluorescence measurements, absorbance of the samples did not exceed 0.05. Therefore, we did not correct the emission intensity for optical filtering effects.

2.4. Analysis of binding data

Results from fluorimetric titrations were analyzed by the following method. Apparent dissociation constant (K_d) was determined using non-linear curve fitting analysis (Eqs. (1) and (2)). All experimental points for binding isotherms were fitted by least-square analysis [21]:

$$K_d = \frac{\left\{C_0 - (\Delta F/\Delta F_{max})C_0\right\}\left\{C_p - (\Delta F/\Delta F_{max})C_0\right\}}{\left\{(\Delta F/\Delta F_{max})C_0\right\}} \quad (1)$$

$$C_0\left(\Delta F/\Delta F_{max}\right)^2 - (C_0 + C_p + K_d)\left(\Delta F/\Delta F_{max}\right) + C_p = 0 \quad (2)$$

ΔF is the change in fluorescence emission intensity of MTR at 540 nm ($\lambda_{ex} = 470$ nm) for each point of the titration curve, ΔF_{max} is the same parameter when the ligand is totally bound to polymer (N-terminal intact/chopped nucleosome core particle/naked DNA), C_p is the concentration of the polymer (N-terminal intact/chopped nucleosome core particle/naked DNA) and C_0 is the initial concentration of the antibiotic. A double reciprocal plot was used for determination of ΔF_{max} using

Eq. (3):

$$\frac{1}{\Delta F} = \frac{1}{\Delta F_{max}} + \frac{K_d}{\{\Delta F_{max}(C_p - C_0)\}} \tag{3}$$

Other details of the method are given in an earlier report [29].

As described in earlier reports [11,29], binding stoichiometry was estimated from the intersection of two straight lines of the least-square fit plot of normalized increase in fluorescence against the ratio of input concentration (in terms of DNA base) of N-terminal intact/chopped core particle/ free DNA and drug.

Binding isotherms for daunomycin were obtained from fluorimetric titration experiments as described by Chaires et al. [32]. Binding data obtained from spectrofluorimetric titrations were cast into the form of Scatchard plot of r/C_f vs. r [33], where r is the number of daunomycin molecules bound per mole of nucleotide and C_f is the molar concentration of the free drug. Non-linear binding isotherms were observed in each case and the data were fitted to a theoretical curve drawn according to the neighbor exclusion binding model [34,35]:

$$\frac{r}{C_f} = K'(1-nr)\left[\frac{1-nr}{1-(n-1)r}\right]^{n-1} \tag{4}$$

where K' is the intrinsic binding constant to an isolated binding site and n is the number of nucleotides occluded by the binding of a single ligand molecule. Values of K' and n were estimated by the least-square fitting of the experimental data to Eq. (4).

2.5. Evaluation of thermodynamic parameters

Thermodynamic parameters, ΔH (van't Hoff enthalpy), ΔS (entropy) and ΔG (free energy), were determined using the following equations [27]:

$$\ln K_{app} = \frac{-\Delta H}{RT} + \frac{\Delta S}{R} \tag{5}$$

$$\Delta G = -RT \ln K_{app} \tag{6}$$

where R and T are the universal gas constant and absolute temperature, respectively. K_{app} $(1/K_d)$ was determined at three different temperatures 10, 20 and 27 °C, respectively. ΔH and ΔS were determined from the slope and intercept of a plot of $\ln(K_{app})$ against $1/T$. ΔG was determined from Eq. (6).

Temperature-dependent spectrofluorimetric titrations were performed for daunomycin to estimate the thermodynamic parameters. Intrinsic binding constants were determined at 10, 20 and 30 °C, respectively. The analysis of the van't Hoff plot $(\ln K_{app}$ vs. $1/T)$ obtained over the temperature range of the study enabled the calculation of ΔH, ΔG and ΔS.

2.6. DNA release monitored by agarose gel electrophoresis

Disruption of N-terminal intact nucleosome core particle by complex I was checked as follows. Two hundred microliters of N-terminal intact nucleosome core particles (348 μM in terms of DNA base) in 10 mM Tris–HCl pH 8.0 and 300 μM MgCl$_2$ were incubated with complex I (69 μM MTR plus 300 μM MgCl$_2$, in the same buffer) for 3 h at 30 °C. Small aliquots of this mixture were loaded into a 1.5% agarose gel and allowed to run at 50 V in 1X TBE buffer (Tris/borate/ EDTA buffer) for 45 min. In the case of N-terminal chopped core particles, the experiment was repeated in the same way except that the concentration of N-terminal chopped nucleosome core particle was 225 μM in terms of DNA base and the concentration of complex was 45 μM in terms of MTR.

In the case of complex II, 200 μl of N-terminal intact core particle (630 μM in terms of DNA base) in 10 mM Tris–HCl pH 8.0 and 4 mM MgCl$_2$ were incubated with complex II (126 μM MTR plus 4 mM MgCl$_2$, in the same buffer) at 30 °C for 3 h. Small aliquots of this mixture were loaded into a 1.5% agarose gel and run for 45 min. For the disruption of N-terminal chopped core, the experiment was repeated in the same way except that the concentration of N-terminal

chopped core particle was 255 μM and the concentration of complex II was 51 μM in terms of MTR. In all cases the control samples contain the same concentration of $MgCl_2$ as complex I or II with no antibiotic.

In the case of daunomycin, the same procedure was followed for the DNA release experiments except the concentrations of daunomycin. Daunomycin concentrations of 104 and 77 μM were used for the experiments with N-terminal intact core (348 μM) and N-terminal chopped core (255 μM), respectively. Here, $MgCl_2$ was absent in the working buffer (10 mM Tris–HCl pH 8.0). One hundred and forty-seven base pair nucleosomal DNA was used as an internal marker to check the DNA release during the disruption process. Concentrations of the nucleosome and ligand(s) were so chosen to ensure complete binding of the ligand(s) to the nucleosome.

3. Results

3.1. Absorption studies

Changes in the absorption spectrum of the MTR complexes, I and II, upon binding to N-terminal intact/chopped nucleosome core particle and naked DNA indicate the formation of complex between them (Fig. 2, panels a and b). The main features of the change are a red shift and broadening of the peak relative to that of the free antibiotic and their complexes. There is a concomitant increase of absorbance in the longer wavelength region. These changes are characteristic of the association of the complexes with DNA [8,9]. Spectra of both complexes bound to N-terminal chopped core particle are similar to those in presence of core DNA stripped of all histones. In contrast, we observe a difference in the spectral features of the complexes bound to core particle with N-terminal tails of histones intact.

3.2. Fluorescence studies

Increase in fluorescence intensity of both complexes upon their association with N-terminal intact/chopped core particle and naked DNA provides the method to evaluate the binding parame-
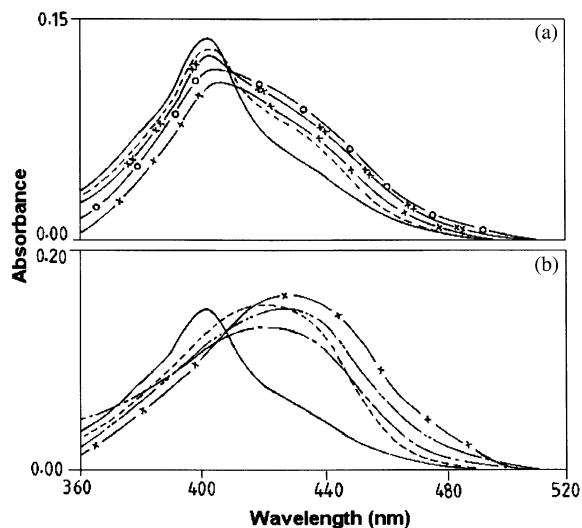

Fig. 2. (a): Absorption spectra (360–520 nm) of MTR (13.5 μM, —) and complex I [MTR (13.5 μM) plus Mg^{2+} (230 μM)] in the absence (– – –) and presence of DNA (350 μM, — o —); N-terminal intact core particle (500 μM, — x —); N-terminal chopped core particle (344 μM, – xx –) in 10 mM Tris–HCl, pH 8.0 at 20 °C. (b): Absorption spectra (360–520 nm) of MTR (13.5 μM, —) and complex II [MTR (13.5 μM) plus Mg^{2+} (2 mM)] in the absence (– – –) and presence of DNA (397 μM, — x —); N-terminal intact core particle (717 μM, — —); N-terminal chopped core particle (520 μM, — - - —) in 10 mM Tris–HCl, pH 8.0 at 20 °C.

ters (Fig. 4). In general, a blue shift of the emission peak accompanies the increase in fluorescence (Fig. 3, panels a and b, Table 1). Increase in the quantum yield and blue shift characterizes the association of both ligands with free DNA [10]. While the blue shift is maximum with naked DNA, its extent is more in case of N-terminal chopped core particle than N-terminal intact core particle. It originates from a change in the local environment and/or conformation of the chromophore in the ligand(s) upon association with nucleosome core particle/free DNA. Fluorescence quantum yield of the bound chromophore is also more in the case of N-terminal chopped core particle compared to N-terminal intact core particle. The increase occurs to a greater degree in the case of the bulkier complex II. Fluorescence quantum yield is greatest when the ligand binds to nucleosomal DNA depleted of histones (Fig. 3,
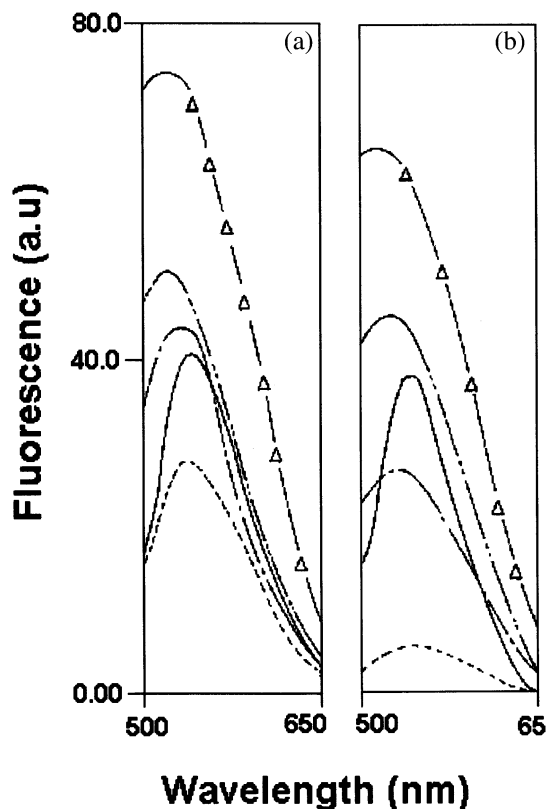
Fig. 3. (a): Fluorescence spectra of MTR (8 μM, —) and complex I [MTR (8 μM) plus Mg^{2+} (230 μM)] in absence (– – –) and presence of DNA (350 μM, — △ —); N-terminal intact core particle (500 μM, — —); N-terminal chopped core particle (344 μM, — -- —) in 10 mM Tris–HCl buffer, pH 8.0 at 20 °C. (b): Fluorescence spectra of MTR (8 μM, —) and complex II [MTR (8 μM) plus Mg^{2+} (2 mM)] in absence (– – –) and presence of DNA (397 μM, — △ —); N-terminal intact core particle (717 μM, — —); N-terminal chopped core particle (520 μM, — -- —) in 10 mM Tris–HCl buffer, pH 8.0 at 20 °C.

panels a and b). In Table 1 we have given a comparison of the blue shift values for both anti-biotics. In general, the blue shift in the fluorescence peak resulting from the association of both complexes of MTR with N-terminal intact/chopped core and DNA depleted of histones is greater than that reported earlier for chromomycin A_3.

In the case of daunomycin there was decrease in the fluorescence intensity without any significant change in the peak position of the ligand on gradual addition of DNA and intact/chopped core (data not shown). The decrease is consistent with an earlier report [31].

3.3. Evaluation of binding parameters

We estimated the binding parameters, binding constant and size of the binding site for the ligand–polymer interaction, from the fluorescence titrations. Representative titration curves for the interaction of complexes, I and II, with different polymers are shown in Fig. 4 (panels a and b). The nature of the curves indicates a non-cooperative binding over the range of input concentrations of polymer. Binding parameters were estimated as described under Section 2. Table 2 summarizes the binding parameters for the interaction of complexes, I and II, with different systems. The main points noted from the table are as follows. Presence of histone proteins in core particle reduces the binding affinity for both complexes, because both complexes bind to the naked DNA with comparatively higher affinity and lower binding site size. Among the N-terminal intact and chopped core particle, the binding affinity is lower in case of the former. There is a considerable increase in the binding affinity after the tryptic removal of N-terminal tail domains. On the other hand, there is a marginal decrease in the binding site size in terms of covered base per drug molecule from N-terminal intact to N-terminal chopped core particle, although the effect is more for bulkier complex II than smaller complex I. Between the two complexes, I and II, the dissociation constant is higher for the bulkier ligand complex II and, as expected, the binding site size is also larger. We have also noticed that the effect of the removal of N-terminal tail domains upon the association parameters of the two complexes depends upon the nature of the antibiotic.

Relevant binding data for the interaction of daunomycin with the polymers are presented in Table 3. Non-cooperative binding isotherms were observed in each case (Fig. 5) and data were fitted to a theoretical curve drawn according to the

excluded site model [35] for a non-linear non-cooperative ligand-binding system using Eq. (3) described in Section 2 (Fig. 5). Daunomycin binds to the naked DNA with comparatively higher affinity. Between the N-terminal intact and chopped core particles, the binding affinity is considerably higher in case of the chopped core. It is comparable to the value for naked DNA. There is no significant change in the binding site size in terms of covered base per drug molecule from N-terminal intact to N-terminal chopped core particle.

3.4. Estimation of thermodynamic parameters

Since the value of dissociation constant at one temperature does not reflect the proper trend in the association with the core particle for the three ligands, we evaluated the associated thermodynamic parameters. Fig. 6a shows the representative van't Hoff plots for the interaction of complexes, I and II, with nucleosome core particle. Thermodynamic parameters are summarized in Table 4. Association with complex I is enthalpy-driven in contrast to the entropy-driven nature of association with complex II.

Table 1
Blue shift in the fluorescence peak of complexes I and II of MTR during their interaction with N-terminal intact/chopped nucleosome core particle and naked DNA in 10 mM Tris–HCl, pH 8.0 at 20 °C

System	ΔF_{max} (nm)
Complex I	
N-terminal intact nucleosome core	6 (3)
N-terminal chopped nucleosome core	16 (12)
Naked DNA	18 (18)
Complex II	
N-terminal intact nucleosome core	16 (15)
N-terminal chopped nucleosome core	24 (21)
Naked DNA	32 (24)

ΔF_{max} is the blue shift in fluorescence peak; values inside the parentheses are for chromomycin A_3.

Removal of N-terminal tail domains culminates in a 2-fold reduction in the contribution of negative enthalpy value for complex I; the negative contribution is compensated by a 10-fold increase in the entropy. The difference in the enthalpy contribution suggests that N-terminal tail domains play a role in the non-covalent interaction with complex I. Removal of N-terminal tails provides better accessibility for complex I to the minor grooves of nucleosomal DNA, as is evident from the greater
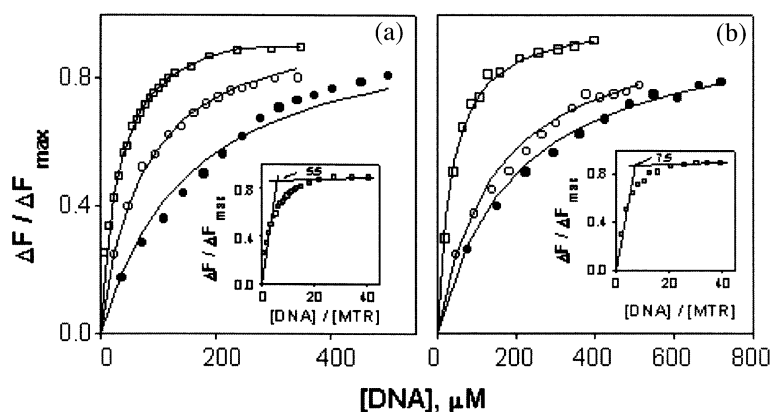

Fig. 4. Curve fitting analyses (plot of normalized increase in fluorescence against the input concentration of polymer) to evaluate the dissociation constant for the association of complex I (panel a) and complex II (panel b) with N-terminal intact core particle (●); N-terminal chopped core particle (○) and naked DNA (□) in 10 mM Tris–HCl buffer, pH 8.0 at 20 °C. Inset in each figure illustrates the method to determine the binding site size, for the association of complexes I or II with naked DNA (□). The abscissa value corresponding to the interaction (shown with the arrow) of the two straight lines gives the value for the binding stoichiometry.

Table 2
Binding parameters for the interaction of MTR–Mg^{2+} complexes with N-terminal intact/chopped nucleosome core particle and naked DNA in 10 mM Tris–HCl buffer, pH 8.0 at 20 °C

System	K_d (μM)	n (base/drug)
Complex I		
N-terminal intact nucleosome core	154 (116)	18 ± 2 (18 ± 2)
N-terminal chopped nucleosome core	72 (85)	13 ± 1.5 (14 ± 1.5)
Naked DNA	33 (54)	5.5 ± 0.5 (6 ± 0.5)
Complex II		
N-terminal intact nucleosome core	201 (210)	38 ± 2.5 (31.8 ± 2.5)
N-terminal chopped nucleosome core	133 (85)	18 ± 0.5 (15.2 ± 0.5)
Naked DNA	32 (20)	7.5 ± 0.5 (7.4 ± 0.5)

The dissociation constant (K_d) and binding site size (n) were calculated as described in Section 2 using the method described in Ref. [29]. The concentration of Mg^{2+} used for the formation of complexes, I and II, was 0.3 and 4 mM, respectively. The data for chromomycin is shown inside the brackets, it has been taken from Ref. [29].

blue shift in the fluorescence peak of complex I as a result of the association with N-terminal chopped core particle. The better accommodation offered by the N-terminal chopped core particle for complex I leads to the displacement of greater number of water molecules from the minor groove. It leads to an increase in the entropy change compared to N-terminal intact nucleosome, because the displaced water molecules contribute to the positive change in entropy.

The situation is radically different for the bulkier complex II; its binding is an entropy-driven process. Removal of N-terminal tails results in an increase in the positive enthalpy value, which is compensated by an increase in the positive entropy. In naked DNA, minor grooves of (G.C) rich regions are freely accessible for the ligands. The bulkier complex II is accommodated in the space of the minor groove via an increase in the groove width accompanied by a B → A type transition in DNA conformation at the binding site [11]. The above explanation for entropy increase is consistent with the proposition that the removal of N-terminal tails enhances accessibility of the ligand to the minor groove of (G.C) rich region. This is also consistent with the trend in the blue shift of fluorescence spectra (Table 2). Association with naked DNA leads to maximum extent in blue shift of the fluorescence peak of complex II.

Differences in the energetics of association between complexes, I or II, of chromomycin A$_3$ and MTR are apparent. The negative enthalpy value is higher for complex I of MTR than that for the same complex of chromomycin A$_3$. After the removal of N-terminal tail domains, there is an increase in the positive entropy value, which is also greater for complex I of MTR. N-terminal tail removal affects the energetics of association for the bulkier complex II to a greater extent in the case of chromomycin A$_3$.

Table 3
Binding parameters for the interaction of daunomycin with N-terminal intact/chopped nucleosome core particle and naked DNA in 10 mM Tris–HCl buffer, pH 8.0 at 20 °C

System	K_d (μM)	n (base/drug)
N-terminal intact nucleosome core	15.2	11.0 ± 0.5
N-terminal chopped nucleosome core	3.1	9.0 ± 0.4
Naked DNA	1.5	10 ± 0.4

The value of dissociation constant, K_d for the binding of daunomycin to the polymer was calculated from the relation; $K_{app} = 1/K_d = K'/n$, where K' is the intrinsic binding constant (in terms of nucleotide) and n is the binding stoichiometry in terms of nucleotide per bound drug. K' and n were obtained from the Scatchard plot as described in Section 2.
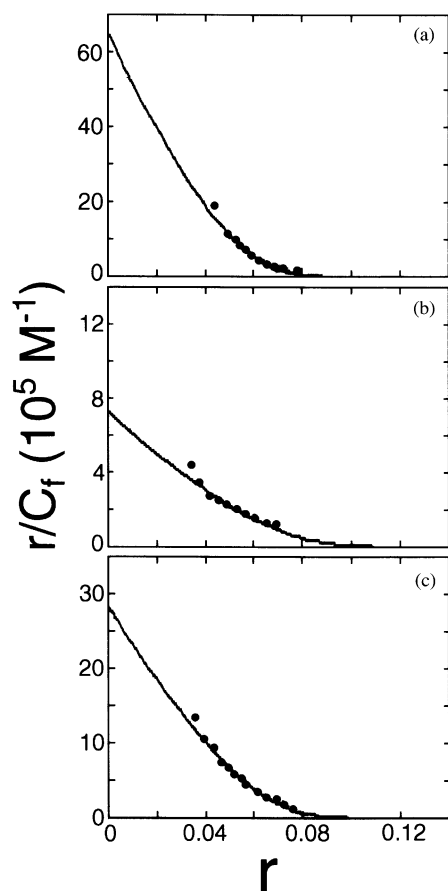
Fig. 5. Representative Scatchard plots for binding of daunomycin to (a) Naked DNA, (b) N-terminal intact nucleosome core particle and (c) N-terminal chopped nucleosome 10 mM Tris–HCl buffer, pH 8.0 at 20 °C. The solid lines are the non-linear least-square best fit of the experimental points to the neighbor exclusion model (Eq. (4)). This model adequately fits the data within the region of the Scatchard plot ranging from 25% (lower limit) and 90% (upper limit). Values of binding parameters are given in Table 3.

A representative van't Hoff plot for the interaction of daunomycin with nucleosome core particles is depicted in Fig. 6b. Thermodynamic parameters are summarized in Table 5. Removal of N-terminal tail domains causes a reduction in the contribution of negative enthalpy value for daunomycin; the negative contribution is compensated by 4-fold increase in the entropy. The better

penetration of the drug in the N-terminal chopped core particle leads to the release of greater number of water molecules from the minor groove. Change in hydration of the N-terminal chopped core particle contributes to the positive change in entropy compared to N-terminal intact nucleosome. It should be noted that we have not performed calorimetry to evaluate the thermodynamic parameters, because for both ligands we noticed a large concentration dependence of the heat of dilution for the ligands.

3.5. CD spectroscopic studies

In order to monitor the effect of N-terminal tail removal upon the binding site environment of both complexes I and II, we have recorded the circular dichroism (CD) spectra of both of them under different conditions. Fig. 7 (panels a and b) shows CD spectra of complexes, I and II, in presence of saturating concentrations of the different polymers. CD spectra of both complexes of MTR are different in the presence of N-terminal intact/chopped
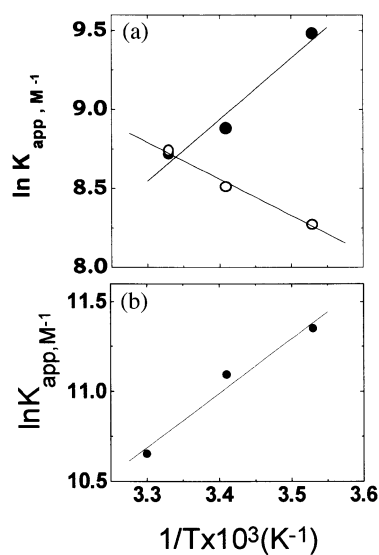

Fig. 6. van't Hoff plots for the interaction of (a) complex I (●) and complex II (○) of MTR and (b) daunomycin (●) with N-terminal intact core particle in 10 mM Tris–HCl buffer, pH 8.0.

Table 4
Thermodynamic parameters for the interaction of complexes, I and II, of MTR with N-terminal intact/chopped nucleosome core particle and naked DNA in 10 mM Tris–HCl buffer, pH 8.0 at 20 °C

System	ΔG (Kcal/mol)	ΔH (Kcal/mol)	ΔS (e.u)
Complex I			
N-terminal intact core particle	−5.1 (−5.3)	−9.8 (−7.7)	−16.0 (−8.1)
N-terminal chopped core particle	−5.5 (−5.5)	−5.9 (−4.8)	−1.4 (2.2)
Naked DNA	−5.9 (−5.7)	−7.5 (−5.2)	−5.5 (1.7)
Complex II			
N-terminal intact core particle	−4.9 (−4.9)	4.6 (2.2)	32.6 (24.2)
N-terminal chopped core particle	−5.3 (−5.5)	5.2 (6.0)	35.7 (39.2)
Naked DNA	−6.0 (−6.3)	3.5 (7.0)	32.3 (45.6)

The concentration of Mg^{2+} used for the formation of complexes, I and II, was 0.3 and 4 mM, respectively. The standard deviation from three sets of experiment is 15%. The values in the parentheses are for chromomycin A_3, as cited from Ref. [29] for comparison.

nucleosome core particle and naked DNA. Changes in the CD spectra of complexes I and II occur as a result of association with DNA in the N-terminal intact and chopped nucleosome core particle. That is why the spectra of both complexes have been recorded in the presence of DNA stripped of histones. In any particular set, CD spectra of the complexes, I or II, pass through a single point at different input concentrations of the polymer (figure not shown). A red shift of the peak in the CD spectra of both complexes upon addition of N-terminal intact/chopped nucleosome/naked DNA is a common feature. Association of complex I with naked DNA results in the loss of parental spectral features; however, the parental spectral features are partially retained during the association with N-terminal intact/chopped core particle. An important feature noted here is the change in CD spectral features of complex I after the removal of N-terminal tail domains. There is hyperchromocity of the positive band during the association of complex I with N-terminal chopped core particle. In contrast, hypochromocity was observed during its association with N-terminal intact core. The trend is reversed in the association of complex I of chromomycin A_3 with N-terminal intact/chopped core particle [29]. The situation is radically different for complex II (Fig. 7, panel b). Here, the differences in spectra upon addition of N-terminal intact/chopped nucleosome core particle and naked DNA are apparent. Association of the complex II with naked DNA results in the loss of parental spectral features; however, the features are partially retained in case of the N-terminal intact/chopped core particle. Interaction of complex II with the N-terminal chopped core particle induces an alteration in the CD spectral features akin to those for the free ligand. There is an increase in the intensity of the positive band of complex II after the removal of N-terminal tail domains. The situation is reversed in case of

Table 5
Thermodynamic parameters for the interaction of daunomycin with N-terminal intact/chopped nucleosome core particle and naked DNA in 10 mM Tris–HCl buffer, pH 8.0 at 20 °C

System	ΔG (Kcal/mol)	ΔH (Kcal/mol)	ΔS (e.u)
N-terminal intact core particle	−6.5	−6.0	1.5
N−terminal chopped core particle	−7.4	−5.2	7.7
Naked DNA	−7.8	−8.6	−2.7

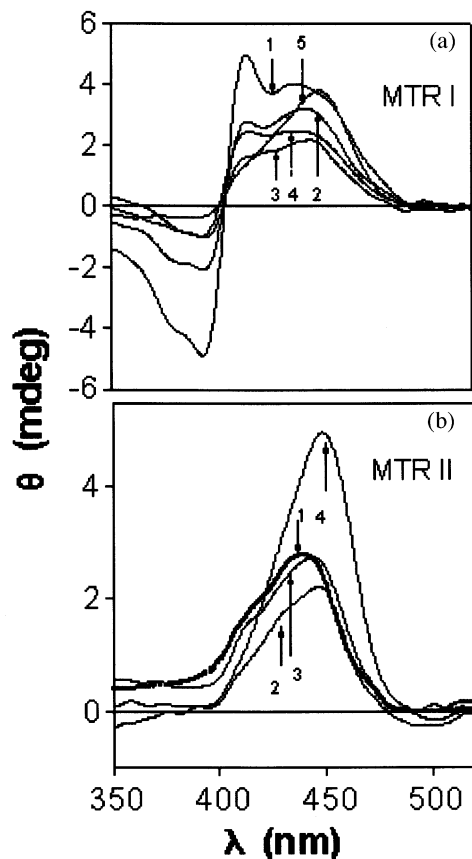The standard deviation from three sets of experiment is 5%.

Fig. 7. CD spectra (350–520 nm) of complexes, I and II, under different conditions in 10 mM Tris–HCl buffer, pH 8.0 at 25 °C: (a) MTR (15 μM) alone (1), complex I [MTR (15 μM) plus Mg^{2+} (230 μM)] (2), complex I in presence of 625 μM of N-terminal intact core particle (3), complex I in presence of 295 μM of N-terminal chopped core particle (4) and complex I in presence of 132 μM of naked DNA (5); (b) complex II [MTR (15 μM) plus Mg^{2+} (2 mM)] (1), complex II in presence of 810 μM of N-terminal intact core particle (2), complex II in presence of 530 μM of N-terminal chopped core particle (3), complex II in presence of 132 μM of naked DNA (4).

chromomycin A_3, where a decrease in the intensity was observed after the tail removal [29]. Overall, the effect of tail removal is more apparent in the CD spectra of both complexes, I and II, of chromomycin A_3 than that of MTR.

The absence of a visible CD band with signifi-

cant molar ellipticity value prevented us from carrying out CD studies with daunomycin.

3.6. Disassembly of nucleosome core structure by complex(es) I and II of mithramycin and daunomycin

We have made an important observation that both complexes of MTR have a tendency to disrupt the nucleosome structure when N-terminal tail domains are removed from the core histones. Fig. 8 (panels a and b) shows the agarose gel electrophoresis of N-terminal intact/chopped core particle in presence and absence of complexes, I and II. From the figure it is clear that complex I can disrupt the N-terminal chopped core particle but is unable to disrupt the N-terminal intact one. As reported earlier, complex I of chromomycin A_3 can disrupt both N-terminal intact and chopped core particles with a preference for N-terminal chopped core [29]. However, the bulkier complex II of MTR (Fig. 8), like the same complex of chromomycin A_3 [29], can disrupt both N-terminal intact and chopped core particles. The effect is relatively more pronounced in the case of N-terminal chopped core particles.

Fig. 9 represents the agarose gel electrophoresis of N-terminal intact/chopped core particle in the presence and absence of daunomycin. From the figure it is observed that daunomycin disrupts both N-terminal intact and chopped core particles. Compared to the groove binder MTR, the extent of DNA release from the disruption of N-terminal chopped core particle by the intercalator daunomycin is greater. From the data it is clear that release of nucleosomal DNA from the nucleosome core depends on the mode of binding of the ligands. It also appears that N-terminal tail domains have a role in maintaining the structural integrity of histone–DNA complex in the nucleosome core particle.

4. Discussion

Two approaches are usually taken to study the effect of the association of DNA-binding anticancer drugs upon the nucleosome. The first one is
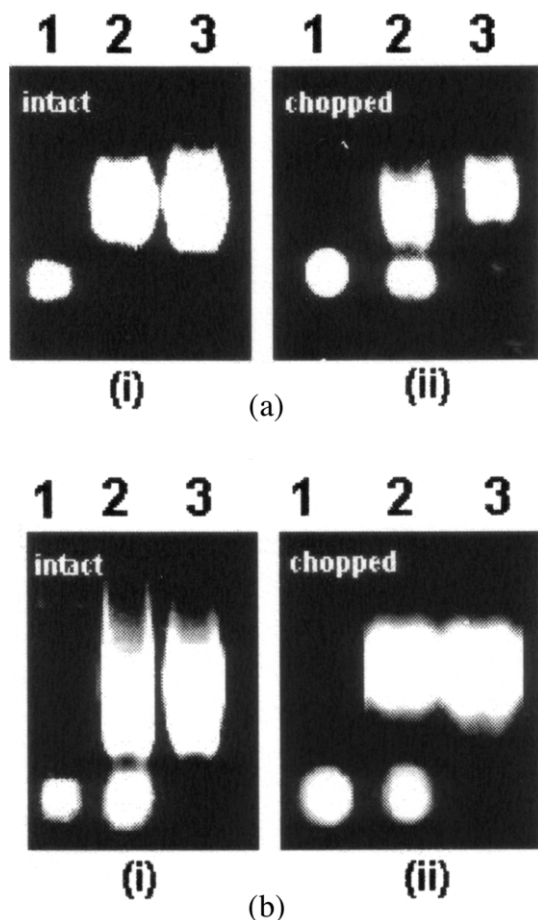
Fig. 8. Agarose gel electrophoresis of the N-terminal intact core particle (i) and N-terminal chopped core particle (ii) in the absence and presence of complex I (a) and complex II (b). Different lanes contain the following samples 147 base pair DNA marker (lane 1), N-terminal intact/chopped core particle in presence of complex I or II (lane 2), N-terminal intact/chopped core particle in absence of complex I or II (lane 3). Concentrations of the complexes and core particles along with the detailed of experimental conditions are given in Section 2.

reconstitution of the model nucleosome in the presence of the drugs. This has been reported earlier in the case of MTR [8,12]. Here, we have taken the second approach of comparing the association of the anticancer drugs with isolated nucleosome under different conditions.

Earlier we reported the effect of N-terminal tail domains upon the accessibility to chromomycin

A_3. Here, we have extended our studies to the clinically employed antibiotics, MTR and daunomycin. Two major conclusions follow the results. The inhibitory role of N-terminal tail domains of the core histones upon the access of small DNA-binding ligands to nucleosomal DNA appears to be a common phenomenon. Removal of the N-terminal domain enhances the accessibility of the small ligands to nucleosomal DNA. Simultaneously, it leads to an enhancement of the extent of
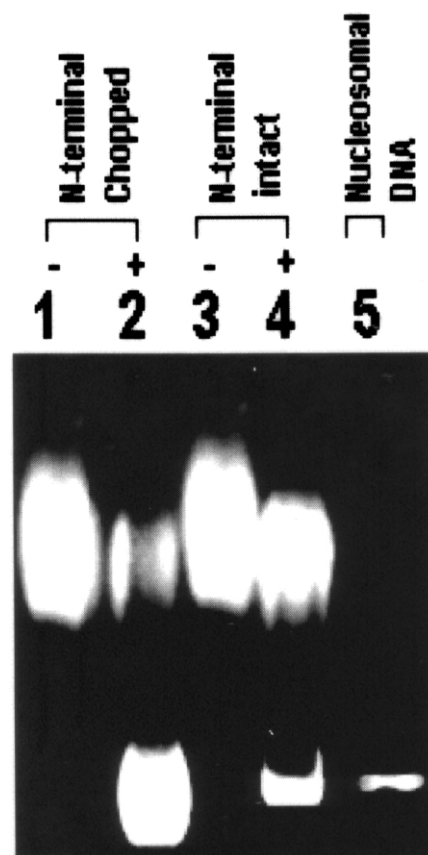

Fig. 9. Agarose gel electrophoresis of the N-terminal chopped core particle, N-terminal intact core particle and nucleosomal DNA in the absence and presence of daunomycin. Different lanes contain the following samples. N-terminal chopped core particle in absence (lane 1) and in presence (lane 2) daunomycin. N-terminal intact core particle in absence (lane 3) and in presence (lane 4) daunomycin. One hundred and forty seven base pair nucleosomal DNA (lane 5). Concentrations of the drug and core particles along with the detailed of experimental conditions are given in Section 2.

nucleosomal disruption by these ligands. Both factors could be potential sources of the transcription inhibitory property of these compounds when the chromatin enters into a transcriptionally active state. Our results also show that the degree to which the above phenomena take place depends upon the mode of interaction of the ligands, namely, groove binding or intercalation, with nucleosomal DNA. In the present report we notice that they are more pronounced with an intercalator than a groove binder. It can be structurally ascribed to a differential extent of relaxation of the superhelical structure of the nucleosomal DNA by the DNA-binding ligands. Our results also imply that binding of the transcription inhibitor leading to structural disassembly and the resultant DNA release would lead to the loss of the chromosomal DNA as templates in the first step of expression of a gene.

We have observed that neither of the two ligands binds with any histone. Independent experiments using the fluorescence properties of the antibiotics have shown the absence of such an interaction. The conclusion from the analysis of binding parameters for both complexes, I and II, of MTR and daunomycin with core particles and naked DNA is that histone–DNA contacts and N-terminal tail domains of individual core proteins in nucleosome core particle reduce the accessibility of (G.C) rich region of nucleosomal DNA to both antibiotics. Between the two complexes, the effect is more pronounced with the bulkier complex, II. Similar trends characterizes the association of chromomycin A_3 with nucleosome core particle [29].

In accordance with our previous report, differences in the spectroscopic features (absorbance, fluorescence and CD) of the MTR complexes bound to N-terminal intact/chopped nucleosome core and naked DNA may be ascribed to dissimilar binding site environment and/or geometry of target DNA in the three systems. Comparison of the CD spectral features of the bound ligands, complexes I and II, supports the proposition that among N-terminal intact and chopped core particles, depletion of the N-terminal tail leads to an alteration in the electronic environment of the bound ligands. However, the effect of tail removal upon the intensity of the positive band in the CD spectra

of both complexes of MTR and chromomycin A_3 are opposite, though they have the same chromophore responsible for spectral transitions in the visible region. This might be postulated as being due to the difference in the nature of the substituents at the sugars of the two antibiotics. The sugar residues in the chromomycin A_3 are more substituted; as a result $CHR-Mg^{2+}$ complexes have less structural flexibility [36]. We have shown this from other studies with linear DNA. This is a potential source for the difference. It implies that sugar residues of the antibiotics play a role in the nucleosome core recognition property of the antibiotics and its in vivo function.

Associated thermodynamic parameters further reinforce the proposition that N-terminal tail domains influence the interaction of MTR and daunomycin with nucleosome. Removal of N-terminal tail domains leads to a behavior more akin to naked DNA for both the drugs (Tables 2 and 3). We also observed a marked difference in the thermodynamic data between MTR and daunomycin supporting our suggestion that the effect of tail removal upon the energetics of association is more apparent for daunomycin. It originates from the fact that tails of histone proteins prevent the access of the planar ring system in daunomycin for intercalation between the DNA base pairs.

Agarose gel electrophoretic experiments have shown that both complexes of MTR have a tendency to disrupt the nucleosome structure. The disruption is dependent upon the concentration of MTR and follows a very slow kinetics with a half-life in the order of hours (results not shown). We suggest that N-terminal chopped nucleosome is more susceptible to disruption by an external groove binder like MTR compared to N-terminal intact nucleosomes. A similar trend characterizes the nucleosome disruption potential of the complexes, I and II, for both CHR and MTR. Complex II is more efficient. Complex I of MTR, a smaller ligand, disrupts the N-terminal chopped nucleosome but is incapable of disrupting the N-terminal intact nucleosome. Comparison of the disruption potentials for the groove binder and intercalator indicates that instability occurs to a greater degree when the ligand binds via intercalation. The extent of disruption is significantly more for the N-

terminal chopped nucleosome core compared to the intact one, thereby further supporting our proposition that N-terminal tail domains have an important role in maintaining the structural integrity of the nucleosome probably by preventing the access of anticancer drugs MTR and daunomycin to the nucleosomal DNA.

5. Conclusion

Summing up the present results along with earlier work [29], we propose that the N-terminal domain of histone might partially stand in the way of access of small ligands to nucleosomal DNA. Another important conclusion is that removal of the N-terminal tail leads to an increase in the ligand-induced instability of the nucleosome. Both explain the molecular basis of pharmacological property via transcription inhibition potential of these ligands.

References

[1] P. Calabresi, B.A. Chabner, in: (Eds.), The Pharmacological Basis of Therapeutics, Macmillan Publishing Co, NY, 1991, pp. 1209–1263.

[2] S.E. Wohlert, E. Kunzel, R. Machinek, C. Mendez, J.A. Salas, J. Rohr, The structure of mithramycin reinvestigated, J. Nat. Prod. 62 (1999) 119–121.

[3] R.C. Synder, R. Ray, S. Blume, D.M. Miller, Mithramycin blocks transcriptional initiation of the c-myc P1 and P2 promoters, Biochemistry 30 (1991) 4290–4297.

[4] S. Chatterjee, K. Zaman, H. Ryu, A. Conforto, R.R. Ratan, Sequence-selective DNA binding drugs mithramycin A and chromomycin A_3 are potent inhibitors of neuronal apoptosis induced by oxidative stress and DNA damage in cortical neurons, Ann. Neurol. 49 (2001) 345–354.

[5] A. Dimaraco, F. Arcamone, F. Zunino, in: J.W. Corcoran, F.E. Hahn (Eds.), Antibiotics, Mechanism of Action of Antimicrobial and Antitumor Agents, Springer, Berlin, 1975, pp. 101–128.

[6] S. Neidle, G.L. Taylor, Nucleic acid binding drugs. Some conformational properties of the anti-cancer drug daunomycin and several of its derivatives: implications for DNA-binding, FEBS Lett. 107 (1979) 348–354.

[7] I.H. Goldberg, P.A. Friedmann, Antibiotics and nucleic acids, Annu. Rev. Biochem. 40 (1971) 775–810.

[8] B.M. Cons, K.R. Fox, High resolution hydroxyl radical footprinting of the binding of mithramycin and related antibiotics to DNA, Nucl. Acids Res. 17 (1989) 5447–5459.

[9] P. Aich, R. Sen, D. Dasgupta, Role of magnesium ion in the interaction between chromomycin A_3 and DNA: binding of chromomycin A_3–Mg^{2+} complexes with DNA, Biochemistry 31 (1992) 2988–2997.

[10] P. Aich, D. Dasgupta, Role of magnesium ion in mithramycin–DNA interaction: binding of mithramycin–Mg^{2+} complexes with DNA, Biochemistry 34 (1995) 1376–1385.

[11] S. Majee, R. Sen, S. Guha, D. Bhattacharya, D. Dasgupta, Differential interactions of the Mg^{2+} complexes of chromomycin A_3 and mithramycin with poly(dG–dC)×poly(dC–dG) and poly(dG)×poly(dC), Biochemistry 36 (1997) 2291–2299.

[12] M.L. Carpenter, J.N. Marks, K.R. Fox, DNA-sequence binding preference of the GC-selective ligand mithramycin. Deoxyribonuclease-I/deoxyribonuclease-II and hydroxy-radical footprinting at CCCG, CCGC, CGGC, GCCC and GGGG flanked by (AT)n and An×Tn, Eur. J. Biochem. 215 (1993) 561–566.

[13] M.A. Keniry, D.L. Banville, P.M. Simmonds, R.H. Shafer, Nuclear magnetic resonance comparison of the binding sites of mithramycin and chromomycin on the self-complementary oligonucleotide d(ACCCGGGT)$_2$. Evidence that the saccharide chains have a role in sequence specificity, J. Mol. Biol. 31 (1993) 753–767.

[14] M.A. Keniry, E.A. Owen, R.H. Shafer, The three-dimensional structure of the 4:1 mithramycin:d(ACCCGGGT)(2) complex: evidence for an interaction between the E saccharides, Biopolymers 54 (2000) 104–114.

[15] M. Sastry, R. Fiala, D.J. Patel, Solution structure of mithramycin dimers bound to partially overlapping sites on DNA, J. Mol. Biol. 251 (1995) 674–689.

[16] A.H. Wang, G. Ughetto, G.J. Quigley, A. Rich, Interactions between an anthracycline antibiotic and DNA: molecular structure of daunomycin complexed to d(CpGpTpApCpG) at 1.2-A resolution, Biochemistry 26 (1987) 1152–1163.

[17] D.J. Patel, S.A. Kozolowski, J.A. Rice, Hydrogen bonding, overlap geometry, and sequence specificity in anthracycline antitumor antibiotic DNA complexes in solution, Proc. Natl. Acad. Sci. USA 78 (1981) 3333–3337.

[18] J.B. Chaires, Equilibrium studies on the interaction of daunomycin with deoxypolynucleotides, Biochemistry 22 (1983) 4204–4211.

[19] K. Van Holde, J. Zlatanova, G. Arents, E. Moudrianakis, in: S.C.R. Elign (Ed.), Chromatin Structure and Gene Expression, Oxford University Press, Oxford, 1995, pp. 1–26.

[20] K. Luger, A.W. Mader, R.K. Richmond, D.F. Sargent, T. Richmond, Crystal structure of the nucleosome core particle at 2.8 A resolution, Nature 389 (1997) 251–260.

[21] K. Luger, Structure and dynamic behavior of nucleosomes, Curr. Opin. Genet. Dev. 13 (2003) 127–135.

[22] J.C. Rice, C.D. Allis, Histone methylation versus histone acetylation: new insights into epigenetic regulation, Curr. Opin. Cell Biol. 13 (2001) 263–273.

[23] D.Y. Lee, J.J. Hayes, D. Pruss, A.P. Wolffe, A positive role for histone acetylation in transcription factor access to nucleosomal DNA, Cell 72 (1993) 73–84.

[24] L.J. Juan, R.T. Utley, C.C. Adams, M. Vettese-Dadey, J.L. Workman, Differential repression of transcription factor binding by histone H1 is regulated by the core histone amino termini, EMBO J. 15 (1994) 6031–6040.

[25] M.F. Garcia-Ramirez, F. Dong, J. Ausio, Role of the histone 'tails' in the folding of oligonucleosomes depleted of histone H1, J. Biol. Chem. 267 (1992) 19587–19595.

[26] A.P. Akhtar, B. Becker, The histone H4 acetyltransferase MOF uses a C2HC zinc finger for substrate recognition, EMBO Rep. 2 (2001) 113–118.

[27] J.M. Gottesfeld, J.M. Belitsky, C. Melander, P.B. Dervan, K. Luger, Blocking transcription through a nucleosome with synthetic DNA ligands, J. Mol. Biol. 321 (2002) 249–263.

[28] M.A. Mir, D. Dasgupta, Interaction of antitumor drug, mithramycin, with chromatin, Biochem. Biophys. Res. Commun. 280 (2001) 68–74.

[29] M.A. Mir, D. Dasgupta, Association of the anticancer antibiotic chromomycin A_3 with the nucleosome: role of core histone tail domains in the binding process, Biochemistry 40 (2001) 11578–11585.

[30] E. Fibach, N. Binachi, M. Borgatti, E. Prus, R. Gambari, Mithramycin induces fetal hemoglobin production in normal and thalassemic human erythroid precursor cells, Blood, 102 (2003) 1276–1281.

[31] J.B. Chaires, N. Dattagupta, D.M. Crothers, Studies on interaction of anthracycline antibiotics and deoxyribonucleic acid: equilibrium binding studies on interaction of daunomycin with deoxyribonucleic acid, Biochemistry 21 (1982) 3933–3940.

[32] J.B. Chaires, N. Dattagupta, D.M. Crothers, Binding of daunomycin to calf thymus nucleosomes, Biochemistry 22 (1983) 284–292.

[33] G. Scatchard, The attraction of proteins for small molecules and ions, Ann. NY Acad. Sci. 51 (1949) 660–672.

[34] D.M. Crothers, Calculation of binding isotherms for heterogeneous polymers, Biopolymers 6 (1968) 575–584.

[35] J.D. McGhee, P.H. von Hippel, Theoretical aspects of DNA–protein interactions: co-operative and non-co-operative binding of large ligands to a one-dimensional homogeneous lattice, J. Mol. Biol. 86 (1974) 469–489.

[36] S. Chakrabarti, B. Bhattacharyya, D. Dasgupta, Interaction of mithramycin and chromomycin A_3 with d(TAGCTAGCTA)$_2$: role of sugars in antibiotic-DNA recognition, J. Phys. Chem. 106 (2002) 6947–6953.